Computers and Concrete, *Vol. 19, No. 1 (2017) 069-078*
DOI: https://doi.org/10.12989/cac.2017.19.1.069

Effect of presoaking degree of lightweight aggregate on the properties of lightweight aggregate concrete

Chao-Wei Tang*

Department of Civil Engineering & Geomatics, Cheng Shiu University, No. 840, Chengcing Rd., Niaosong District, Kaohsiung City, Taiwan R.O.C.

(Received January 6, 2016, Revised October 17, 2016, Accepted October 21, 2016)

Abstract. This study aimed at exploring the effect of presoaking degree of lightweight aggregate (LWA) on the fresh and hardened properties of concrete. Two series (i.e., Series A and Series B) of concrete mixes that were made of LWA with different moisture states were prepared. The presoaking degree of LWA was divided into three types: oven dry state, 1 hour prewetted and 24 hours prewetted. For the Series A, the water content of the lightweight aggregate concrete (LWAC) mixes was adjusted in accordance with the moisture condition of the LWA. Whereas the amount of water added in the Series B mixes was deliberately not adjusted for the moisture condition of the LWA. Slump test, mechanical tests, interfacial transition zone microscopical tests and thermal conductivity test were carried out on the specimens of different concretes and compared with control normal-weight aggregate concretes. The test results showed that the effect of mixing water absorption by LWA with different moisture states was reflected in the fresh concrete as the loss of mixture workability, while in the hardened concrete as the increase of its strength. With the use of oven-dried LWA, the effect of reduction of water-cement ratio was more significant, and thus the microstructure of the ITZ was more compact.

Keywords: lightweight aggregate; workability; interfacial transition zone; mechanical property

1. Introduction

Lightweight aggregate (LWA) is mainly produced from materials such as clay, shale, slate, or natural deposits and industrial wastes (Somayaji 2001, Tang *et al.* 2011, Tang 2014). The most important aspect of LWA is the porosity. The lightweight of LWA is due to the cellular or high internal porous microstructure, which gives this type of aggregate a low bulk specific gravity (Chandra and Berntsson 2002). LWA with a variety of particle size and particle density levels has been used in the concrete industry for a variety of lightweight aggregate concrete (LWAC). Comparing with normal-weight aggregate concrete (NC), LWAC possesses many advantages such as lightweight, lower thermal conductivity, durability and better seismic resistance (Lo *et al.* 1999, Young *et al.* 2002, Holm *et al*. 2004, Lo *et al.* 2004, Beycioğlu *et al.* 2015, Hwang and Tran 2015, Ji *et al.* 2015, Oktay *et al.* 2015, Tang 2015, Zhang *et al.* 2015, Kabay *et al.* 2016).

The major factors affecting the water absorption of LWA include the particle pore structure and its surface texture. Basically, there are two types of pore in a LWA particle: closed-pore and open-pore (Chandra and Berntsson 2002). In general, LWAs with a vitrified surface or isolated pores tend to absorb little water, while the one with connected or open pores will be able to absorb more water into the pore structure because of capillary absorption (Bogas *et al.* 2015, Franus *et al.* 2016). On average, LWAs usually absorb more water than their normal-weight aggregate counterparts. Based upon a 24-hour absorption test conducted in accordance with the procedures of ASTM C 127 and ASTM C 128, structural-grade LWAs will absorb from 5% to more than 25% moisture by mass of dry aggregate (BE96-3942/R20 2000). By contrast, ordinary aggregates generally absorb less than 2% of moisture. The important distinction in stockpile moisture content is that with LWA the moisture is largely absorbed into the interior of the particles, while with ordinary aggregates it is primarily surface moisture (Holm *et al.* 2004).

In view of the high level of water absorption of LWA particles, it is necessary to adopt a modified approach to concrete proportioning. For instance, slump loss in LWAC can be an acute problem because of the water absorption of the LWA particles. This can be alleviated by presoaking the LWA before batching. The water absorption of LWA after presoaking treatment is weakened, and thus the fluidity of the mixture can be effectively improved. Soaking LWA for 24 hours prior to mixing is the most commonly used in laboratory applications, while soaking the aggregates is not very practical in field applications (Golias *et al.* 2012). In particular, the presoaking time of LWA will affect the actual water-cement ratio in a concrete mixture, and thus affecting the fresh and hardened properties of LWAC. The problem of water-cement ratio reduction in LWAC because of mixing water absorption by the LWA has attracted the attention of many scholars (Punkki and Giørv 1993, Sandvik and Hammer 1995, Smeplass *et al.* 1995, Lo *et al.* 2008, Golias *et al.* 2012, Domagała 2015, Zaichenkoa, Lakhtarynaa *et al.* 2015). In addition, some LWAC production guidelines

*Corresponding author, Professor
E-mail: tangcw@gcloud.csu.edu.tw

ISSN: 1598-8198 (Print), 1598-818X (Online)

Table 1 Chemical composition and physical properties of cement

Chemical composition (%)		Physical properties	
Silicon dioxide, S_iO_2	20.9	Specific gravity	3.15
Aluminum oxide, Al_2O_3	5.65	Specific surface area (cm^2/g)	3400
Iron oxide, Fe_2O_3	3.21	Loss on ignition (%)	0.92
Calcium oxide, C_aO	63.63	Insoluble residue (%)	0.11
Magnesium oxide, M_{gO}	2.25	Soundness (%)	0.055
Sulfur trioxide, SO_3	2.16	7-Day Compressive strength (MPa)	35.5
Sodium oxide, Na_2O	0.1	28-Day Compressive strength (MPa)	46.3
Potassium oxide, K_2O	0.52		
Tricalcium silicate, C_3S	48.76		
Dicalcium silicate, C_2S	23.14		
Tricalcium aluminate, C_3A	9.54		
Tetracalcium aluminoferrite, C_4AF	9.77		

Table 2 Physical and mechanical properties of LWA

Particle density (g/cm^3)	1-hour Water absorption (%)	24-hour Water absorption (%)	Crushing strength (MPa)
1.22	4.21	7.70	10.1

Table 3 Mix proportions and slump results for concrete

	Mix No.	w/c	Cement (kg/m^3)	Water (kg/m^3)	SP (kg/m^3)	FA (kg/m^3)	CA (kg/m^3)	Slump (cm)
Series A	N50-A	0.50	392	196	1.57	728	497	12
	T0L55-A	0.55	450	248	0	604	427	9
	T1L52-A	0.52	450	235	0	618	473	11
	T24L50-A	0.50	450	223	0	630	515	11
Series B	N50-B	0.50	373	187	0	880	877	8
	T0L50-B	0.50	373	187	0	880	416	5
	T1L50-B	0.50	373	187	0	880	416	6
	T24L50-B	0.50	373	187	0	880	416	8

Notes: w/c=Water/cement ratio, SP=Superplasticizer, FA=Fine aggregate, CA=Coarse aggregate

recommend the use of oven-dried aggregates or the one with initial moisture limited to the amount of water that will be absorbed by the aggregate within 30 minutes up to 1 hour (Domagała 2015).

In response to the above statements, this research aims to investigate the effect of LWA presoaking duration on the fresh and hardened properties of LWAC. A series of experiments had been conducted, including mechanical property tests (i.e., compressive strength, elastic modulus, splitting tensile strength and flexural strength), micro property tests (i.e., microscopic hardness and pore volume content) and thermal property tests (i.e., thermal conductivity). The experimental parameters include the presoaking time of LWA, water-cement ratio, and curing age.

2. Experimental details

2.1 Experimental program

The water absorption and desorption behavior of LWA in concrete matrix is a dynamic balance process, and its intensity depends on particle porosity, moisture content after presoaking, matrix consistency and degree of cement hydration. In this study, the impact of the initial moisture condition of the LWA on the fresh and hardened properties of concrete was evaluated. Two types of concretes were made: LWAC and NC, the latter serving as the reference concrete. Two series (i.e., Series A and Series B) of LWAC mixes that were made of LWA with different moisture states were prepared. The presoaking degree of LWA is divided into three types: oven dry state, 1 hour prewetted and 24 hours prewetted. The drying and presoaking of LWA was applied prior to mixing. First, dry the representative samples of LWA to constant weight at a temperature of 110±5°C (approximately 24 hours). Then the samples were allowed to cool for 24 hours. Subsequently, immerse the samples in water at room temperature for a period of targeted time.

For the Series A, the water content of the LWAC mixes was adjusted in accordance with the absorption capacity of the aggregates. As a result, the Series A mixes were developed with variable water-cement ratio (0.50 to 0.55 by mass). Whereas the water-cement ratio and cement content in the Series B mixes were kept constant at 0.50 and 373 kg/m^3, respectively. In other words, the water content was deliberately not adjusted to explore the impact of moisture condition of LWA on the properties of concrete. Slump test, mechanical tests, interfacial transition zone microscopical tests and thermal conductivity test were carried out on the specimens of each concrete mixture and compared with the reference concretes.

2.2 Materials

Materials used for making specimens included cement, fine aggregates and coarse aggregates. The cement used here was Type I Portland cement manufactured by Taiwan Cement Corporation with a specific gravity of 3.15 and a fineness of 3400 cm^2/g. The chemical composition and physical properties of the cement are listed in Table 1. The lightweight coarse aggregate is a synthetic aggregate manufactured from fine sediments collected from the Shihmen Reservoir in Taiwan. Its physical and mechanical properties are listed in Table 2. As can be seen in Table 2, the crushing strength of the LWA was 10.1 MPa, which was measured by compressing the aggregates in a steel cylinder through a prescribed distance of 20 mm in accordance with GB2842-81 (GB/T2842-81, China National Standard Test method for lightweight aggregates).

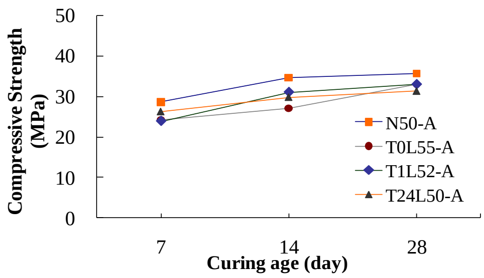

(a) Series A

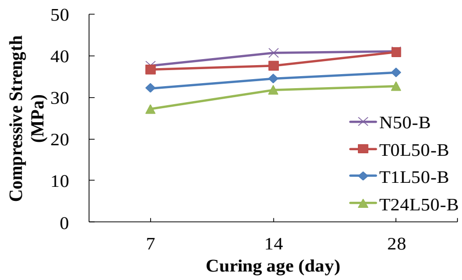

(b) Series B

Fig. 1 Compressive strength of concrete versus curing age

2.3 Mix proportions and casting of specimens

Table 3 presents the mix proportions for both types of concrete (i.e., NC and LWAC). For the Series A, the specified 28-day compressive strengths were chosen equal to 30 MPa. For example, N50-A is for normal-weight concrete. The normal-weight fine aggregate was natural river sand with a specific gravity of 2.59 and a fineness modulus of 2.58. Prior to mixing, the LWA was presoaked in water for 0, 1, and 24 hours, respectively. As shown in Table 3, T0L55-A is for the Series A LWAC with oven-dried LWA; T1L52-A is for the Series A LWAC with LWA presoaked in water for 1 hour; T24L50-A is for the Series A LWAC with LWA presoaked in water for 24 hours. The normal-weight coarse aggregate was crushed stone with a specific gravity of 2.60 and a maximum particle size of 19 mm. For the Series B, the normal-weight coarse aggregate was crushed stone with a specific gravity of 2.53 and a maximum particle size of 19 mm. The normal-weight fine aggregate was natural river sand with a specific gravity of 2.64 and a fineness modulus of 2.79.

All aggregates were cured in a room until the required condition was reached. The treated aggregates were then stored in a room in which the ambient temperature and relative humidity (RH) were controlled at 25±3°C and 50±5% to prevent moisture changes. In mixing, the cement, fine aggregates, and coarse aggregates were generally blended first, and then water and superplasticizer (if any) were added. The mixing continued until a uniform concrete without any segregation was obtained.

Concrete specimens for each test were cast out of each mixture and compacted using an external vibrator. Along with each mixture, nine 100 mm in diameter×200 mm in high cylindrical specimens were cast for compressive strength test and elastic modulus test; nine 150 mm in diameter×300 mm in high cylindrical specimens were also cast to determine the splitting tensile strength of concrete; nine prism specimens (3600 mm in length×100 mm in width×100 mm in thickness) were cast for flexural strength of concrete. Following casting, all the specimens were covered overnight with a wet hessian and polyethylene sheets for a period of 24 hours. After 24 hours, the specimens were removed from the molds. To maintain the same environmental conditions, all specimens were placed in a water bath in the laboratory. After curing, the specimens were removed from the water bath one day before the test.

2.4 Testing methods

The tests of compressive strength, elastic modulus, splitting tensile strength and flexural strength for concrete were performed according to ASTM C39, ASTM C469, ASTM C496 and ASTM C78 standards, respectively.

The porosity and pore size distribution in the interfacial transition zone (ITZ) between cement paste and aggregate was measured by mercury intrusion porosimetry (MIP). The samples for the MIP tests were extracted from the fracture pieces at the core of the cylindrical specimens after the compression test. The fragments without coarse aggregate were dipped into methanol to avoid rehydration immediately after being crushed and were dried in the vacuum desiccators for 2 days. Then treatment by distilled in glass type methanol were adopted to not change the porosity and pore size distribution and to stop hydration of cement before the MIP tests. As the injection pressure on the mercury gradually increases, mercury is forced into the pores on the surface of the sample at incremental pressures; at each step the intruded volume is measured. The pressure of mercury intrusion porosimeter ranges from 1.4 to 414 MPa. The pressure required is a function of the pore size and can be converted to equivalent pore width using the Washburn equation (Galle 2001). Then two important parameters related to the pore structure of the samples can be extracted from the cumulated pore volume versus pore diameter graphs, i.e., threshold pore size and total pore volume.

Moreover, the method of X-ray diffraction (XRD) was adopted to investigate the changes of material properties in the cement paste; the scanning electron microscopy (SEM) observation, energy dispersive spectroscopy (EDS) analysis and microhardness test were used to assess the feature of the ITZ in concrete; the thermal conductivity of the specimens was measured in accordance with the regulations of ASTM C177-13 (2013) to assessment the thermal capacity of concrete.

3. Experimental results and discussion

3.1 Slump test results

For the Series A, as previously stated, the water content of the LWAC mixes was adjusted in accordance with the moisture condition of the aggregates. With different degrees of presoaked LWA, the water-cement ratio of mix

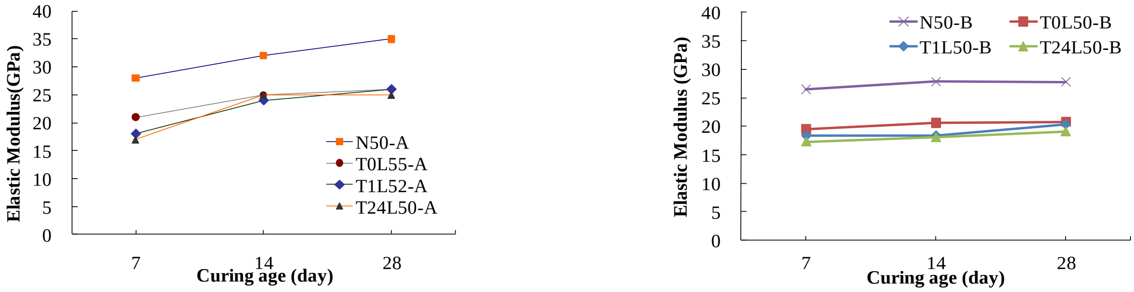

(a) Series A (b) Series B

Fig. 2 Elastic modulus of concrete versus curing age

proportions for each LWAC is also different. It can be seen from Table 3 that the results of the slump tests ranged between 9 cm and 11 cm. Under the condition of the water-cement ratio of 0.50, owing to the low density of the LWA, the slump for T24L50-A is lower than that of the control group (N50-A), but the difference between them it is not significant. The result shows that the use of LWA presoaked in water for 24 hours can ensure better workability of LWAC. Further, in the experimental group, although the water-cement ratio for T0L55-A is highest, its slump value is lowest because of the use of oven-dried LWA. Judging from this, the use of LWA without presoak will absorb the moisture from the cement paste, resulting in lower concrete slump. As for T1L52-A and T24L50-A, they have the same slump value. This shows that adjusting the amount of mixing water in accordance with the moisture condition of the LWA can result in the same slump.

As for the Series B, the mix proportions were designed to maintain a nominal fixed water-cement ratio (0.50). In particular, the mixing water was deliberately not adjusted in accordance with the moisture condition of the aggregates. Owing to high water absorption of the LWA, the actual water-cement ratio was lower than its nominal value. On the whole, absorption by the LWA significantly decreased the workability of concrete mixture. It can be seen from Table 3 that the results of the slump tests ranged between 5 cm and 8 cm. Overall, because of using a low water-cement ratio (0.50), the slump of the Series B is significantly lower than that of the Series A. Likewise, owing to the low density of the LWA, the slumps for T0L50-B and T1L50-B are lower than that of the control group (N50-B); especially T0L50-B with LWA without presoaking process, it has the lowest value of slump. However, T24L50-B with LWA presoaked in water for 24 hours and normal-weight concrete (N50-B) can maintain the same slump. This situation is similar to the comparison between T24L50-A and N50-A in the Series A concrete mix. In summary, the effect of mixing water absorption by LWA with different moisture states was reflected in the fresh concrete as the loss of mixture workability.

3.2 Compressive strength test results

Compression testing was performed using a servo-hydraulic material testing system. Mean compressive strength was calculated by taking average of three specimens. The mean compressive strength versus curing age for the LWAC and NC is shown in Fig. 1. On the whole, absorption by the LWA significantly decreases the workability, whereas it increases the strength, in particular, the early strength.

For the Series A, the 28-day compressive strengths ranged from 31 to 35 MPa. Fig. 1(a) shows that the compressive strength increased with the increase of curing age of concrete, and the compressive strength of the control group (N50-A) is the highest for all types of curing age. In addition, the compressive strength in the experimental group (LWAC) is about 10% to 25% less than that of the control group (NC). Among the mix proportions for the LWAC, T0L55-A has the lowest 7- and 14-day compressive strengths. This may be due to its relatively higher water-cement ratio. Furthermore, the use of oven-dried LWA in T0L55-A will absorb the moisture from the cement paste, thus affecting its cement hydration, resulting in lower strength. As for 28-day compressive strength, although the water-cement ratio and aggregate presoaking degree for each LWAC are different, the magnitudes of compressive strength for each mix proportion are similar. In other words, there is no significant difference in strength between each mix proportion.

For the Series B, the 28-day compressive strengths ranged from 32 to 41 MPa. It can be seen from Fig. 1(b) that the compressive strength also increased with the increase of curing age of concrete, and the compressive strength of the control group (N50-B) is the highest for all types of curing age. In general, the compressive strength of the experimental group was about 0% to 25% less than that of the control group; wherein the compressive strength of T0L50-B was the highest, T24L50-B was the lowest. This shows that the shorter the presoaking time of the LWA, the higher was the resulting strength. The reason is the actual water-cement ratio reduced owing to mixing water absorption by the LWA. The water absorption capacity of oven-dried LWA in T0L50-B is the strongest, thus resulting in a stronger cement matrix. In other words, the effect of mixing water absorption by LWA was reflected in the hardened concrete as the increase of its strength. In summary, for the Series B, the compressive strength of LWAC is closely related to the presoaking degree of LWA.

3.3 Elastic modulus and Poisson's ratio test results

The elastic modulus versus curing age for both the

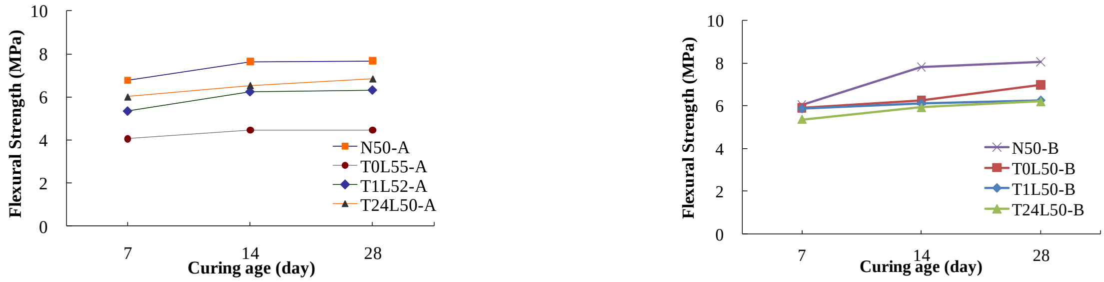

(a) Series A (b) Series B

Fig. 3 Flexural strength of concrete versus curing age

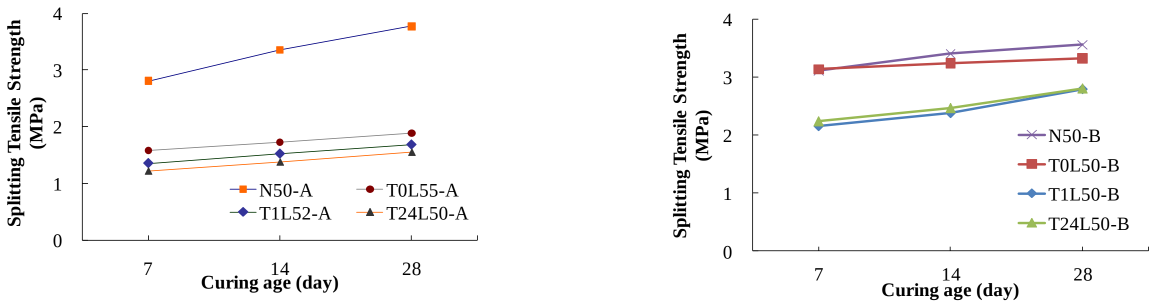

(a) Series A (b) Series B

Fig. 4 Splitting tensile strength of concrete versus curing age

Table 4 Poisson's ratio results for concrete

Mix No.	Poisson's ratio		
	7-Day	14-Day	28-Day
N50-A	0.20	0.25	0.22
T0L55-A	0.32	0.30	0.25
T1L52-A	0.29	0.33	0.31
T24L50-A	0.30	0.40	0.30

control group and the experimental group is shown in Fig. 2. In general, the change of elastic modulus with increasing age was consistent with the results of the compressive strength. For the Series A, it is clear from Fig. 2(a) that as the curing age increased, the elastic modulus of the experimental group increased, but their magnitudes were significantly lower than that of the control group (about 34% to 40% lower). In addition, the elastic modulus for each mix substantially increased with increasing curing age from 7 to 14 days. For the Series B, Fig. 2(b) shows that the elastic modulus of the LWAC was also significantly lower than that of the control group (about 27% to 35% lower); wherein the elastic modulus for T0L50-B was the highest, T24L50-B was the lowest. In view of this, concrete structures made of LWAC will display a higher elastic deformation. That is to say, once LWAC members are under load, their deformation will be far greater than NC. Further, at 28 days age, whether Series A or Series B, the effect of LWA presoaking on the elastic modulus of LWAC is not significant.

Table 4 shows that the Poisson's ratios for LWAC in the Series A were significantly higher than those of the control group; in addition, at 28 days' age, the Poisson's ratios for LWAC with presoaking LWA is relatively higher.

3.4 Flexural strength test results

For the Series A, the flexural strength of the experimental group ranged from 4 to 6 MPa for all types of curing age. It is clear from Fig. 3(a) that as the curing age increased, the flexural strength of the experimental group increased, but their magnitudes were significantly lower than that of the control group (about 12% to 42% lower). Moreover, the flexural strength for each mix clearly increased with increasing curing age from 7 to 14 days. However, for T0L55-A with a higher water-cement ratio, the strength growth is relatively slow, and the magnitude of strength is much lower than those of the other LWAC. This result shows that the flexural strength of LWAC with oven-dried LWA is significantly lower than those of the LWAC with presoaked LWA. In other word, the effect of reduction of water-cement ratio is not significant.

For the Series B, the flexural strength of the experimental group ranged from 5 to 6.5 MPa for all types of curing age. Fig. 3(b) shows that the flexural strength of the experimental group increased roughly with increasing curing age from 7 to 28 days. In addition, the flexural strength of the LWAC was lower than that of the control group (about 0% to 26% lower); wherein the flexural strength for T0L50-B was the highest, T24L50-B was the lowest, but there is no significant difference between T0L50-B and T24L50-B. The results show that owing to the effect of reduction of water-cement ratio, the flexural strength of LWAC with oven-dried LWA is no less than those of the LWAC with presoaked LWA. The results differ from the Series A. The reason may be related to the use of different types of fine aggregate in each series of LWAC.

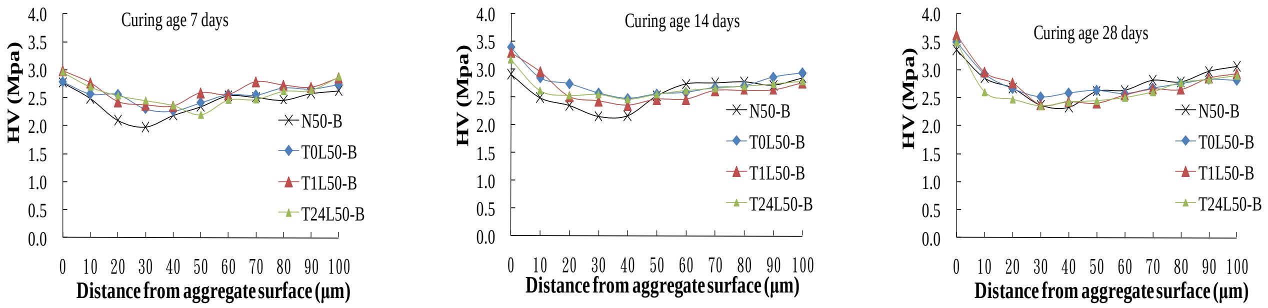

(a) 7-Day (b) 14-Day (c) 28-Day

Fig. 5 Microhardness of concrete versus curing age

Table 5 Relative peak intensity results for concrete

Mix No.	Relative peak intensity (%)(2θ=34.09°)		
	7-Day	14-Day	28-Day
N50-B	11.7	14.3	19.2
T0L50-B	10.7	11.6	15.7
T1L50-B	14.6	15.8	20.8
T24L50-B	14.8	14.6	19.2

Note: In silicon (2θ=26.6°) the peak intensity was 100% to calculate the relative peak intensity of CH (2θ=34.09°)

3.5 Splitting tensile strength test results

For the Series A, the splitting tensile strength of the experimental group ranged from about 1 to 2 MPa for all types of curing age. It is clear from Fig. 4(a) that as the curing age increased, the splitting tensile strength of the experimental group increased, but their magnitudes were significantly lower than that of the control group (about 40% to 50% lower). Moreover, the splitting tensile strength of T0L55-A is a little higher than those of the other LWAC. This result shows that the strength increase is significant because of the effect of reduction of water-cement ratio.

As for the Series B, Fig. 4(b) shows that as the curing age increased, the splitting tensile strength of the experimental group increased. The splitting tensile strength of the experimental group ranged from 2 to 3 MPa for all types of curing age, which are higher than those of the experimental group in the Series A. The reason is the water-cement ratio of the Series B is lower than that of the Series A. In addition, the splitting tensile strength of T0L50-B was lower than that of the control group (about 0% to 7% lower); while the splitting tensile strength of T1L50-B and T24L50- B was about 22% to 31% lower than that of the control group. The results show that the splitting tensile strength of LWAC with oven-dried LWA is much better than those of the LWAC with presoaked LWA. In other words, owing to the effect of reduction of water-cement ratio, the strength increase is very significant.

3.6 Microhardness test results

The microhardness value (referred to as HV) versus curing age for the Series B is plotted in Fig. 5, where each data is the average of 10 test points. In Fig. 5, the vertical axis refers to the HV and the horizontal axis refers to the distance from the aggregate surface. It can be seen that the HV of the ITZ area for each mix is generally increased with an increase in the curing age. In addition, it can be seen that, a compact ITZ area is formed around LWA, its HV is significant higher than that of the bulk cement paste and the ITZ area around dry LWA has the highest HV. This is due to the infiltration of paste into the surface pores of the lightweight aggregate to a certain depth. Thus the two can be closely integrated.

On the other hand, the HV of the ITZ area for both LWAC and NC is different. Basically, the formation of HV distribution for the LWAC is a smoother curve, representing less obvious weak zone; its width is about 30-40 μm. By contrast, the hardness profile for the NC shows an obvious minimum value, roughly forming a notch upward curve. In other words, there is an obvious weak zone; its width is about 45-50 μm. In the experimental group, T0L55-B with oven-dried LWA shows a smoother curve. Owing to the strong absorption capacity of the oven-dried LWA, there is no bleeding phenomenon between aggregate and paste, and thus reducing the water-cement ratio. As a result, the strength of the ITZ area is relatively strong, so the overall HV is higher than that of the other two mixes (T1L50-B and T24L50-B). This demonstrates that the presoaking degree of the LWA exerts a different influence on the microstructure of the ITZ area. With the use of oven-dried LWA, the effect of reduction of water-cement ratio is more significant, and thus the microstructure of the ITZ is more compact. On the contrary, with the increase of the presoaking time of the LWA, the effect of reduction of water-cement ratio is relatively weak, and thus the improvement effect on the microstructure of the ITZ is not significant. In summary, the high water absorption characteristics of the oven-dried LWA can avoid forming a significant weak zone between the cement paste and aggregate, thus enhancing the strength of the ITZ area. This result confirms the strength increase owing to the effect of reduction of water-cement ratio.

3.7 X-ray diffraction test results

Fig. 6 illustrates the XRD analysis of cement paste for both the LWAC and NC specimens. Each test specimen exhibits calcium hydroxide (CH) crystal, which has XRD peak intensity at 2θ of 34.09° (peak relative intensity as

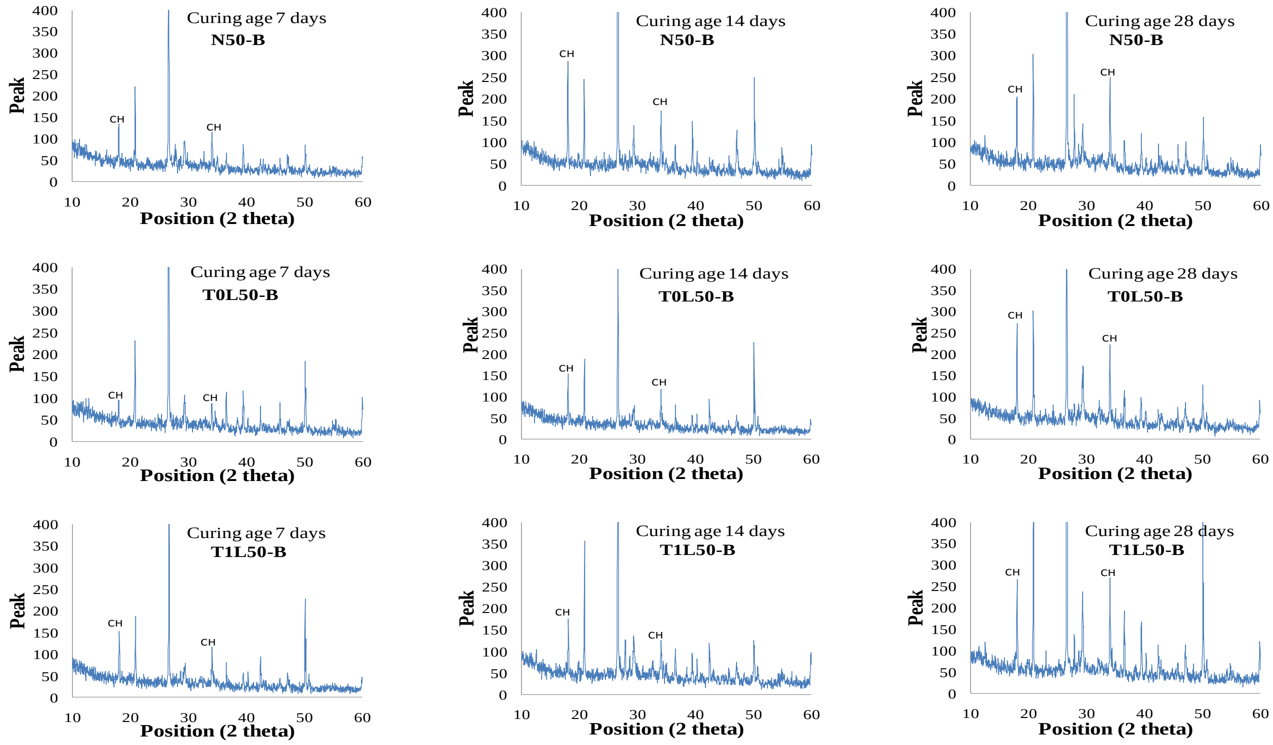

(a) 7-Day (b) 14-Day (c) 28-Day

Fig. 6 X-ray diffraction analysis

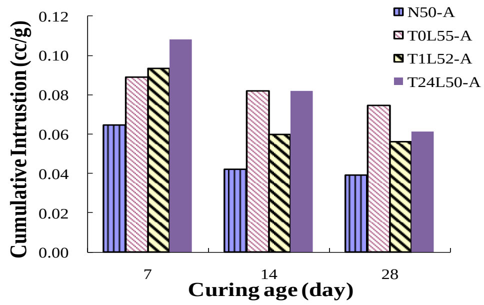

Fig. 7 Cumulative intrusion volume of mercury for cement paste in concrete versus curing age

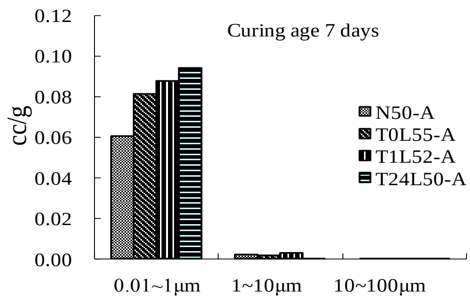

Fig. 8 Cumulative intruded pore volume versus equivalent pore diameter for cement paste in concrete

shown in Table 5). In addition, the content of CH crystal also increased with an increase in the curing age. Fig. 6 shows that the CH content of T0L50-B with oven-dried LWA was the lowest. This is due to the water absorption characteristics of the oven-dried LWA, resulting in free water reduction and lower rates of hydration. As for T1L50-B with LWA presoaked in water for 1 hour, its CH content is higher than that of T0L50-B. In view of this, with the level of X-ray diffraction peak intensity of different curing period LWAC, the semi-quantitative comparison of CH content in the ITZ area of concrete can be done to understand the extent of presoaked LWA on the hydration of the cement paste and to assess the overall micro-structural properties of concrete.

3.8 Microscopic test results

Fig. 7 shows the plots of cumulative intrusion volume of mercury versus curing age for cement pastes in the Series A with different water-cement ratios. It can be seen that the intruded pore volume decreased with increasing curing age from 7 to 28 days. The cumulative amount of porosity at curing age of 7 days in each mix was the highest, which was due to the degree of hydration of the cement at early age was still low, the hydration products failed to fully fill the colloidal pores in the paste. In addition, Fig. 8 shows the cumulative intruded pore volume versus equivalent pore diameter curves for cement pastes in the Series A, in which the equivalent pore diameter was calculated by using the Washburn equation. From Fig. 8, it can be clearly seen that the micropore structure of cement pastes contained mainly capillary porosity and most of the pore radius are ranged from 0.01 to 1 μm. Moreover, it can be observed from Fig. 7 that under the same condition of curing age, the intruded mercury in LWAC is higher than that of NC. The reason is the higher porosity in the paste of LWAC owing to the

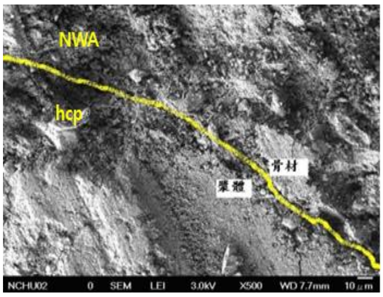

(a) NC (7-Day)

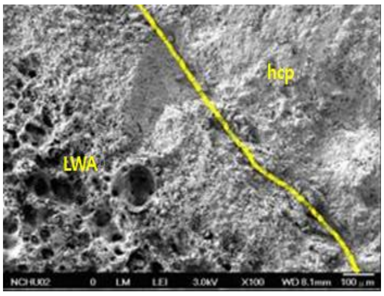

(b) LWAC (7-Day)

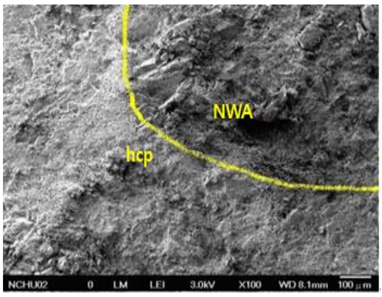

(c) NC (14-Day)

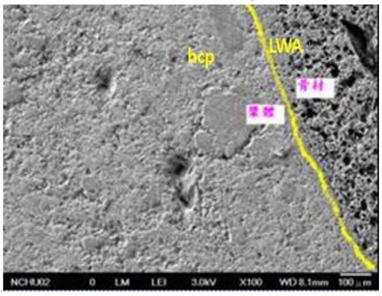

(d) LWAC (14-Day)

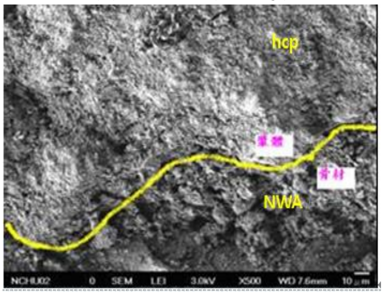

(e) NC (28-Day)

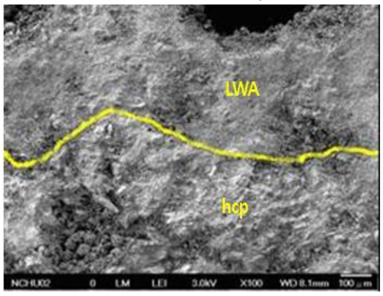

(f) LWAC (28-Day)

Fig. 9 SEM micrographs of interfacial transition zone between cement paste and aggregate

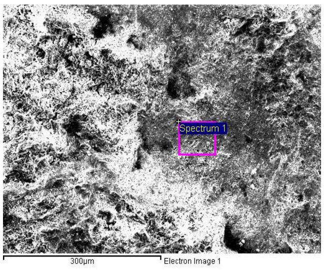
(a) SEM observation for N50-A

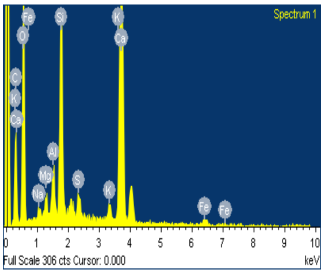
(b) Micro elements in ITZ for N50-A

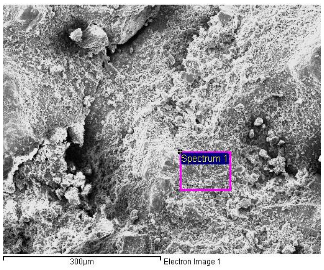
(c) SEM observation for T0L55-A

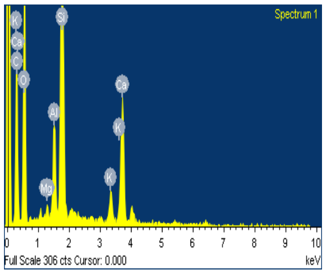
(d) Micro elements in ITZ for T0L55-A

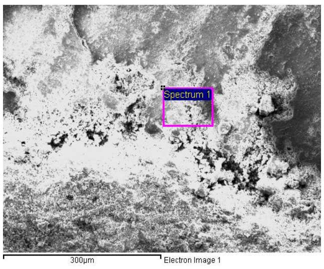
(e) SEM observation for T1L52-A

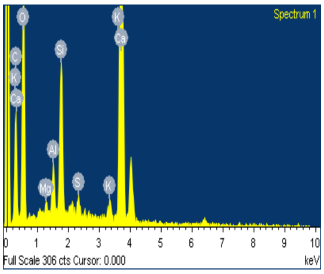
(f) Micro elements in ITZ for T1L52-A

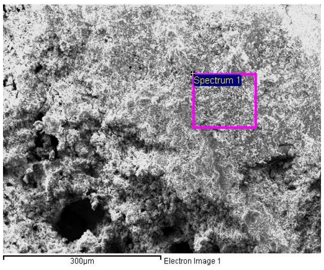
(g) SEM observation for T24L50-A

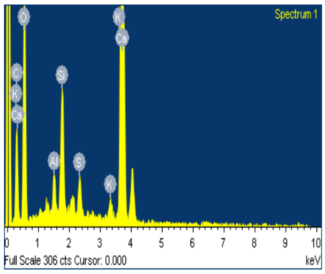
(h) Micro elements in ITZ for T24L50-A

Fig. 10 SEM observation and micro elements in ITZ (28-Day)

amount of mixing water in LWAC is higher. In particular, at curing age of 7 days, the cumulative amount of porosity for T24L50-A was the highest because there is an obvious weak zone; however, its structure became denser with increasing curing age, and thus reducing the intruded mercury. As a result, the cumulative intruded pore volume at curing age of 28 days for T24L50-A is even lower than that of T0L55-A. From this perspective, the use of LWA presoaked in water for 24 hours could easily lead to a concrete with high porosity at early ages. But, owing to internal curing effect of the LWA, the porosity of the LWAC can be reduced at later ages.

On the other hand, the SEM observation test was used to investigate the differences in the microstructure of the Series A. Fig. 9 and Fig. 10 show the characteristic images of the microstructure obtained from the SEM/EDS observations for the two types of analyzed specimens. Compared with ordinary aggregate, the role of LWA and hardened cement paste (hcp) is completely different. In addition, the microstructure of interface area is also different. The cement paste penetrated the surface pores of the LWA, thereby providing a good mechanical interlocking after hardening between the LWA and paste. From Fig. 9, it can be observed that the boundary between the cement matrix and the LWA shell is not distinct, which shows the LWA bonds more tightly and continuously with

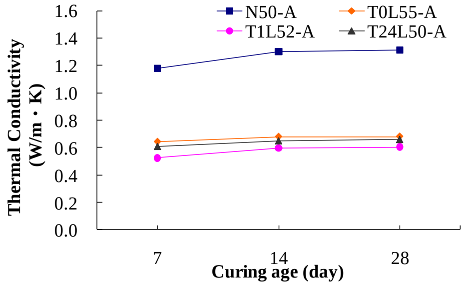

(a) Series A

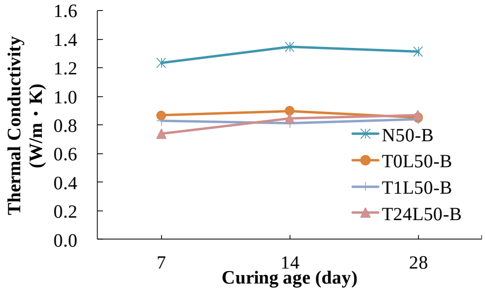

(b) Series B

Fig. 11 Thermal conductivity versus curing age

the cement matrix. The well-bonded interfacial zone is a characteristic of higher strength development of the LWAC.

Furthermore, it can be seen from Fig. 9 that whether LWAC or NC, there are many micro-cracks in the ITZ area between hcp and aggregate, which are the main cause for the formation of weak zone. Overall, the ITZ area between aggregate and hcp is quite obvious at early ages. In addition, the micro-cracks in the ITZ area of NC are mainly around the aggregate surface, while the micro-cracks in the ITZ area of LWAC are some distance away from the aggregate surface. The reason is the normal-weight aggregates with a dense texture are not easy to absorb water so that a layer of water accumulates around aggregate particles (the so-called Wall Effect), increasing the water-cement ratio in its surrounding cement paste and leading to micro-cracks in the ITZ area. By contrast, the rough surface texture and pore structure of the LWA makes it relatively easy for water to be absorbed, decreasing the water-cement ratio in its surrounding cement paste and showing a denser matrix, thus making the distribution of micro-cracks in the rear of the dense matrix.

Moreover, the spectrum of the chemical composition of the main phase formed during the maturation of the cement paste is shown in Fig. 10. The results show that the proportion of cement paste composition varies with the presoaking time of LWA. According to the EDS analysis, calcium, silicon, and oxygen are the main elements, which can yield the conclusion that calcium silicate hydrate (C-S-H colloid), calcium hydroxide (CH), ettringite (Aft) and monosulfate (Afm) were the main hydration products for both the LWAC and NC specimens. In particular, C-S-H colloid plays an important role on the strength of hcp.

3.9 Thermal conductivity test results

Fig. 11 shows the plots of thermal conductivity versus curing age for specimens of both LWAC and NC. Overall, the thermal conductivity of the experimental group ranged from 0.52 to 0.90 W/m·K for all types of curing age. Because of porous structure in LWA, the thermal conductivity of the LWAC was superior to that of the NC.

On the other hand, it can be observed from Fig. 11 that the thermal conductivity roughly increased with the increase of curing age. The reason is that thermal conductivity of the concrete will increase with increasing curing age owing to the decreased pore volume. Moreover, at different curing ages, the effect of different presoaking degree of LWA on thermal conductivity is not significant.

4. Conclusions

The effect of LWA presoaking on the properties of LWAC specimens was described and compared with companion NC specimens. Based on the experimental results, the following conclusions can be drawn:

- The effect of mixing water absorption by LWA with different moisture states was reflected in the fresh concrete as the loss of mixture workability. The longer the presoaking time of the LWA, the better was the resulting workability.
- The effect of mixing water absorption by LWA was reflected in the hardened concrete as the increase of its strength. The shorter the presoaking time of the LWA, the higher was the resulting strength.
- The effect of presoaking degree of LWA on the properties of LWAC is depending on the concrete mix proportions. The reason may be related to the water-cement ratio and the use of different types of fine aggregate in each series of LWAC.
- With the use of oven-dried LWA, the effect of reduction of water-cement ratio is more significant, and thus the microstructure of the ITZ is more compact. On the contrary, with the increase of the presoaking time of the LWA, the effect of reduction of water-cement ratio is relatively weak, and thus the improvement effect on the microstructure of the ITZ is not significant.
- With the level of X-ray diffraction peak intensity of different curing period LWAC, the semi-quantitative comparison of CH content in the ITZ area of concrete can be done to understand the extent of presoaked LWA on the hydration of the cement paste and to assess the overall micro-structural properties of concrete.
- The rough surface texture and pore structure of the LWA makes it relatively easy for water to be absorbed, decreasing the water-cement ratio in its surrounding cement paste and showing a denser matrix.

Acknowledgments

The author expresses his gratitude and sincere appreciation to the Ministry of Science and Technology, Taiwan, for financing this research work.

References

ASTM C177-13 (2013), *Standard Test Method for Steady-State Heat Flux Measurements and Thermal Transmission Properties by Means of the Guarded-Hot-Plate Apparatus*, ASTM International, West Conshohocken, PA.

ASTM C496-96 (1996), *Standard Test Method for Splitting Tensile Strength of Cylindrical Concrete Specimens*, ASTM International, West Conshohocken, PA.

ASTM C469/C469M-14 (2014), *Standard Test Method for Static Modulus of Elasticity and Poisson's Ratio of Concrete in Compression*, ASTM International, West Conshohocken, PA.

ASTM C39/C39M-14a (2014), *Standard Test Method for Compressive Strength of Cylindrical Concrete Specimens*, ASTM International, West Conshohocken, PA.

ASTM C78/C78M-10 (2010), *Standard Test Method for Flexural Strength of Concrete (Using Simple Beam with Third-Point Loading)*, ASTM International, West Conshohocken, PA.

BE96-3942/R20 (2000), *The Effect of the Moisture History on the Water Absorption of Lightweight Aggregates*, EuroLightCon.

Beycioglu, A., Arslan, M.E., Bideci, O.S., Bideci, A. and Emiroglu, M. (2015), "Bond behavior of lightweight concretes containing coated pumice aggregate: Hinged beam approach", *Comput. Concrete*, **16**(6), 909-918.

Bogas, J.A., Gomes, M.G. and Sofia Real, S. (2015), "Capillary absorption of structural lightweight aggregate concrete", *Mater. Struct.*, **48**(9), 2869-2883.

Chandra, S. and Berntsson, L. (2002), *Lightweight Aggregate Concrete*, Noyes Publications, New York, U.S.A.

Domagała, L. (2015), "The effect of lightweight aggregate water absorption on the reduction of water-cement ratio in fresh concrete", *Proc. Eng.*, **108**, 206-213.

Franus, M., Barnat-Hunek, D. and Wdowin, M. (2016), "Utilization of sewage sludge in the manufacture of lightweight aggregate", *Environ. Monit. Assess*, **188**(1), 10.

Galle, C. (2001), "Effect of drying on cement-based materials pore structure as identified by mercury intrusion porosimetry-A comparative study between oven-, vacuum-, and freeze-drying", *Cement Concrete Res.*, **31**(10), 1467-1477.

GB/T2842-81 (1981), *Test Method for Lightweight Aggregates*, China National Standard.

Golias, M., Castro, J. and Weiss, J. (2012), "The influence of the initial moisture content of lightweight aggregate on internal curing", *Constr. Build. Mater.*, **35**, 52-62.

Holm, T.A., Ooi, O.S. and Bremner, T.W. (2004), *Moisture Dynamics in Lightweight Aggregate and Concrete*, Expanded Shale Clay & Slate Institute.

Hwang, C.L. and Tran, V.A. (2015), "A study of the properties of foamed lightweight aggregate for self-consolidating concrete", *Constr. Build. Mater.*, **87**, 78-85.

Ji, T., Zheng, D.D., Chen, X.F., Lin, X.J. and Wu, H.C. (2015), "Effect of prewetting degree of ceramsite on the early-age autogenous shrinkage of lightweight aggregate concrete", *Constr. Build. Mater.*, **98**, 102-111.

Kabay, N., Kizilkanat, A.B. and Tüfekçi, M.M. (2016), "Effect of prewetted pumice aggregate addition on concrete properties under different curing conditions", *Period. Polytech. Civil Eng.*, **60**(1), 89-95.

Lo, Y., Gao, X.F. and Jeary, A.P. (1999), "Microstructure of pre-wetted aggregate on lightweight concrete", *Build. Environ.*, **34**(6), 759-764.

Lo, Y., Cui, H.Z. and Li, Z.G. (2004), "Influence of aggregate prewetting and fly ash on mechanical properties of lightweight concrete", *J. Waste Manage.*, **24**(4), 333-338.

Lo, Y., Cui, H.Z., Tang, W.C. and Leung, W.M. (2008), "The effect of aggregate absorption on pore area at interfacial zone of lightweight concrete", *Constr. Build. Mater.*, **22**(4), 623-628.

Oktay, H., Yumrutas, R. and Akpolat, A. (2015), "Mechanical and thermophysical properties of lightweight aggregate concretes", *Constr. Build. Mater.*, **96**, 217-225.

Punkki, J. and Giørv, O.E. (1993), "Water absorption by high-strength lightweight aggregate", *Proceedings of the Symposium of Utilization of High Strength Concrete*, Lillehammer, Norway, 20-23.

Sandvik, M. and Hammer, T.A. (1995), "The development and use of high performance lightweight aggregate concrete", *Proceedings of the Congress Structural Lightweight Aggregate Concrete*, Sandefjord, Norway, 617-627.

Smeplass, S., Hammer, T. and Sandvik, M. (1995), "Production of structural high strength LWAC with initially dry aggregates", *Proceedings of the Congress Structural Lightweight Aggregate Concrete*, Sandefjord, Norway, 390-396.

Somayaji, S. (2001), *Civil Engineering Materials*, Prentice Hall, Upper Siddle River, New Jersey, U.S.A.

Tang, C.W., Chen, H.J., Wang, S.Y. and Spaulding, J. (2011), "Production of synthetic lightweight aggregate using reservoir sediments for concrete and masonry", *Cement Concrete Compos.*, **33**(2), 292-300.

Tang, C.W. (2014), "Producing synthetic lightweight aggregates by treating waste TFT-LCD glass powder and reservoir sediments", *Comput. Concrete*, **13**(2), 149-171.

Tang, C.W. (2015), "Local bond stress-slip behavior of reinforcing bars embedded in lightweight aggregate concrete", *Comput. Concrete*, **16**(3), 449-466.

Young, J.F., Mindess, S. and Daewin, D. (2002), *Concrete*, Prentice-Hall, Inc., Upper Saddle River, New Jersey, U.S.A.

Zaichenkoa, M., Lakhtarynaa, S. and Korsunb, A. (2015), "The influence of extra mixing water on the properties of structural lightweight aggregate concrete", *Proc. Eng.*, **117**, 1036-1042.

Zhang, J., Wang, J. and Han, Y. (2015), "Simulation of moisture field of concrete with pre-soaked lightweight aggregate addition", *Constr. Build. Mater.*, **96**, 599-614.

CC